Journal of Nano- and Electronic Physics
Vol. **15** No 2, 02026(4pp) (2023)

Журнал нано- та електронної фізики
Том **15** № 2, 02026(4cc) (2023)

Impact of Annealing Temperature on Surface Reactivity of ZnO Nanostructured Thin Films Deposited on Aluminum Substrate

Zehira Belamri[1,*], Warda Darenfad[2], Noubeil Guermat[3]

[1] *Laboratory of Phase Transformation, University Frères Mentouri of Constantine 1, 25000 Constantine, Algeria*
[2] *Thin Films and Interfaces Laboratory (LCMI), University of Constantine 1, 25000 Constantine, Algeria*
[3] *Department of Electronics, Faculty of Technology, University Mohamed Boudiaf of M'sila, 28000 M'sila, Algeria*

(Received 05 February 2023; revised manuscript received 16 April 2023; published online 27 April 2023)

In the present work, the fabrication of a hydrophobic surface was carried out by thermal oxidation of thin layers of Zn deposited by electrodeposition on an aluminum substrate under air atmosphere at different temperatures between 400 °C and 500 °C. Structural analysis by XRD and Raman spectroscopy shows that increasing the annealing temperature leads to the formation of a considerable amount of ZnO on the aluminum substrate. ZnO-bound XRD peaks appear and Zn- and Al-bound peaks decrease. For T_S = 400 °C and 500 °C, the films treated at are polycrystalline with a hexagonal structure of the Wurtzite type due to the existence of the more intense peak relating to the orientation (100) located around the angle 31.75 °. EDX analysis gives the chemical composition of these films and confirms the presence of zinc and oxygen in an almost stoichiometric composition. The morphological study of thin layers treated at 500 °C shows the coexistence of nanostructures in the form of deformed flowers, which leads to their hydrophobicity. The contact angle values measured are > 90° for the films treated at 400 °C and 500 °C, which confirms the hydrophobic nature with a high value obtained equal to 135°.

Keywords: ZnO nanostructures, Electrodeposition, Deformed flowers, Contact angle, Hydrophobic.

DOI: 10.21272/jnep.15(2).02026 PACS number: 81.15.Pq

1. INTRODUCTION

Semiconductor materials based on metal oxides have been of great interest for several decades and in particular in their nanostructured forms, for applications in nanosciences and nanotechnologies [1, 2]. Among all types of metal oxides, zinc oxide (ZnO) has attracted increasing interest in the fabrication of many devices, including gas sensors [3], solar cells and photovoltaic [1, 2]. Its morphology is easily modified by the addition of dopants, the nature of the substrate, the elaboration technique and the annealing temperature. The appearance of the films can vary from a smooth and compact surface to a very rough surface which exhibits a hydrophobic character. The concept of preparing these surfaces presents enormous opportunities in the field of corrosion inhibition of metals and alloys. Superhydrophobic surfaces are an important parameter to characterize surface wettability, characterized by high hydrophobicity, where water drops flow down the surface with a contact angle greater than 150° and can easily slide over the surface, that is i.e. a small contact angle hysteresis [4]. The superhydrophobic ZnO films were obtained by combining the roughness of the surface with the low value of the surface energy. This superhydrophobicity stabilizes ZnO against harsh corrosive environments such as acidic or basic solutions and even high temperatures [5]. These superhydrophobic surfaces have a wide field of applications. They can be used, for example, to protect the antennas of snow houses that stick to them and can interfere with signal reception [6]. St Gobain markets self-cleaning windows which reduce the time and cost of cleaning. These surfaces are also used to make anti-plow textiles such as umbrellas. The rough micro/nanostructured surface state and a non-polar surface chemistry are the two main properties to trap air and reduce attractive interactions between the solid surface and the liquid [7]. Structural defects and growth changes of nanostructured ZnO are sensitive to Raman spectroscopy [8]. Several physical and chemical deposition methods are used to prepare thin layers of ZnO. Among the processes for producing thin layers of zinc oxide, our choice fell on the electrodeposition process. The many advantages offered by this process (does not require an ultra-high vacuum medium, is inexpensive and makes it possible to prepare materials at temperatures close to ambient) justify the choice of this method.

The objective of this present work is to study the effect of the annealing temperature on the structural, morphological and wettability properties of zinc oxide (ZnO) for fabricate hydrophobic thin films on an aluminum metal substrate.

2. EXPERIMENTAL DETAILS

The aluminum substrate undergoes mechanical polishing until a flat shape and a thickness of 2 mm are obtained before deposition of the Zn layer. For cleaning this substrate, it undergoes ultrasonic cleaning for 15 minutes in successive baths, one containing distilled water and the other ethanol. To prepare the starting solution for the deposition of Zn thin films, initially, zinc acetate ($Zn(CH_3CO_2)_2$) powder was dissolved in distilled water. The concentrations of the precursor solution are 0.2 M. Aluminum substrate as cathode and platinum as anode were vertically immersed in the prepared solution and kept at a distance of 1.5 cm. –10 V DC was applied for 15 minutes at room temperature. After deposition, the Zn films are thermally oxidized at 500 °C for 2 h.

* belamri.zehira@umc.edu.dz

To characterize the present phases and their orientations, a PANALYTICAL Empyrean diffractometer (XRD, Cu Kα radiation, $\lambda = 1.540$ Å) was used. HORIBA LabRAM HR Evolution type spectrometer was used to register the Raman spectra at room temperature with a monochromatic radiation source of 473 nm. The morphological and elemental analyses were performed using a Field Emission Gun Scanning Electron Microscope (SEM, Jeol FEG JSM-7100 F) equipped with an energy dispersive X-ray spectrometer (EDX). Contact angle measurements were carried out at room temperature using an optical system composed of a lamp delivering white light and projecting the image of the drop deposited on the sample (LEYBOLD type light source (6 V, 30 W)).

3. RESULTS AND DISCUSSION

3.1 X-Ray diffraction study

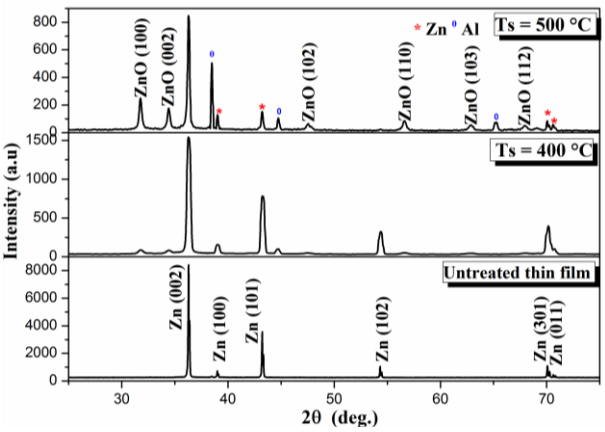

Fig. 1 – X-ray diffraction spectra of layers treated at different annealing temperatures (*time* = 2 h)

Fig. 1 shows the typical X-ray diffraction spectra of a sample of ZnO deposited at room temperature and annealed for two temperatures equal to 400 °C and 500 °C with a fixed *time* = 2 h. On the same Fig. it is not clear that the diffraction peaks relating to Zn, before treatment, the orientations (002) and (101) are dominant, no peak relating to ZnO, was observed. Similar results were obtained by Bouhssira et al. [9]. This absence of the Zn-O bond is due to the presence of oxygen at interstitial sites in the film [9]. With the increase in the annealing temperature (Ts), we clearly see the emergence of peaks relating to zinc oxide which appear to the detriment of that of zinc. At 500 °C there is a decrease in the zinc peaks and the appearance of the aluminum peak corresponds to the aluminum substrate with the presence of six (6) ZnO diffraction peaks located at 31.75°, 34.41°, 47.56°, 56.62° and 69.98° are assigned to either the (100), (002), (102), (112), (103) and (200) planes, respectively. This indicates that 500 °C is the critical temperature for the transformation of Zn into ZnO, which allows better crystallization and organization of the crystal lattice. In addition, the elaborate layers are polycrystalline with a hexagonal structure of the Wurtzite type due to the existence of the more intense peak relating to the orientation (100) located around the 31.75° angle. Moreover, the ZnO films thus produced have a preferential orientation (100) as in the case for the spray pyrolysis method [10, 11].

Fig. 2 shows the variation of the (100) peak of a ZnO thin film as a function of the annealing temperature. There is an increase in the intensity and sharpening of the peak when the annealing temperature increases from 400 °C to 500 °C, which is reflected by an increase in the crystallite size (Table 1).

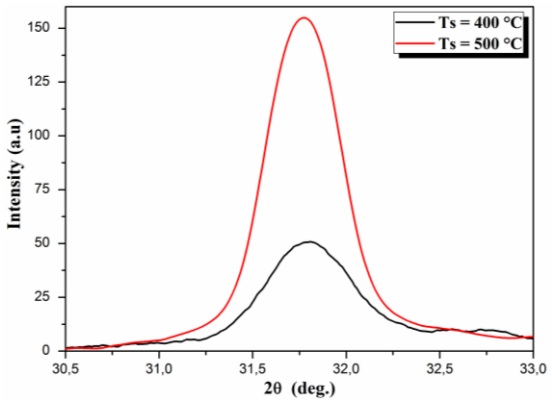

Fig. 2 – Peak position (100) of X-ray diffraction and their intensities films treated at different annealing temperatures 400 °C and 500 °C

The crystallite size (D) of the peak (100) were calculated from the Debye-Scherrer formula [12]:

$$D = \frac{0.9\lambda}{\beta \cos\theta}, \qquad (1)$$

where, λ is the wavelength of X-rays radiation, β represents the full width at half maximum (FWHM) and θ is the angle of diffraction.

Table 1 summarizes the values of the full width at half maximum, the crystallites size and the intensity of layers treated at different annealing temperatures 400 °C and 500 °C.

Table 1 – Variation of the full width at half maximum, the crystallite size and the intensity of our films.

Sample	Crystallite size, (nm)	FWHM	Intensity
400 °C	19.529	0.42317	51.01
500 °C	21.324	0.3875	154.49

The values of the full width at half maximum (FWHM) change inversely with the crystallite size (Table 1). As can be seen, the variations of FWHM and the crystallite size are very well correlated. We have an increase in the crystallite size of our films from 19.529 nm to 21.324 nm as a function of *Ts* between 400 °C and 500 °C, respectively. This increase is probably explained by the improvement in the crystal quality of the layer, as shown by the XRD spectrum (Fig. 1). Similar observation was reported by Quiñones-Galván et al. [13]. In addition, higher temperature improved the adhesion of thin films on the Aluminum substrate.

3.2 Raman Spectroscopy Study

Raman spectroscopy was used in this present work to complete the structural properties study of the elaborated ZnO thin films. The identification of the different vibration modes of the crystal lattice leads to the determination of the different phases of the studied material.

Raman spectroscopy was also used to determine the stress state present in the studied material by observing the peak position displacement in comparison with the values of the material in its bulk state. In this present work, commercial ZnO powder is used as a reference.

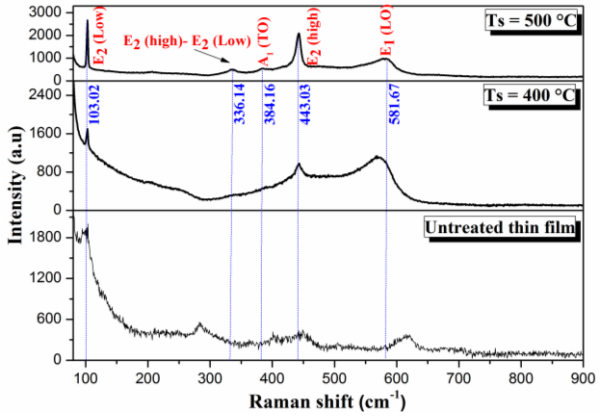

Fig. 3 – Raman spectra of ZnO thin films deposited on Aluminum substrates at various annealing temperatures

The obtained spectrum of the studied sample treated for 2 h at 500 °C is similar to that of massive ZnO and consists of five peaks corresponding to the E_2^{low}, E_2^{high}-E_2^{low}, A_1(TO), E_2^{high}, and A_1(LO)/E_1(LO) modes of the ZnO phonons of hexagonal structure (Fig. 3). All of these peaks can exist with varying intensities depending on the treatment temperature; peak intensities are more noticeable in the spectrum of the sample treated at 500 °C. the two spectra present two intense peaks; the first around 100 cm^{-1}, which corresponds to the E_2^{low} mode associated with the vibration of the zinc atom lattice [14, 15], and the second around 443 cm^{-1}, which corresponds to the E_2^{high} mode, which is attached to the vibration of the sub-lattice of oxygen atoms in the ZnO crystal [16, 17]. These are two representative modes of wurtzite ZnO structure with good crystalline quality, especially for the treated sample at 500 °C.

3.3 Morphology and Wettability Study

Fig. 4 (a) shows the Field Emission Scanning Electron Microscopy (FESEM) images of ZnO thin films obtained with a thermal oxidation of 2 h at 500 °C. The morphology shows that this layer has a repeated distribution of the deformed flower-shaped structures (conical shape), which are covered with a large number of the spherical ZnO nanostructures. The EDS results revealed that the films were made up of Zinc, oxygen and carbon (Fig. 4 (b)). The presence of carbon (C) may come from the aluminum substrate.

The measures of the static contact angles (CA) were made on all ZnO films deposited in aluminum substrate treated at 400 °C and 500 °C for an ambient temperature (27 °C) and a constant humidity rate. In order to reduce the evaporation of the distilled water drop as much as possible, all CA measurements are made after 5 seconds with a fixed *volume* = 5 µl deposited using a micropipette. The gout images are captured by a video camera (Fig. 5). We check the measurements of each film treated (400 °C or 500 °C) by depositing at least four drops of liquid in different places of the surface.

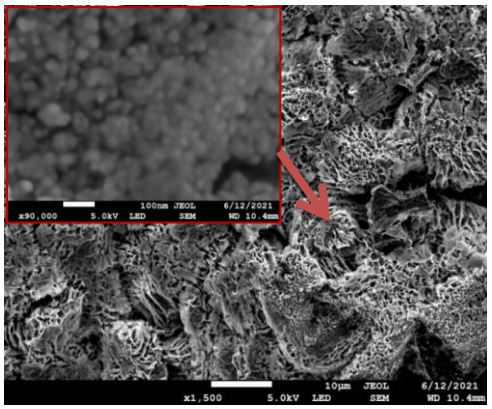

a

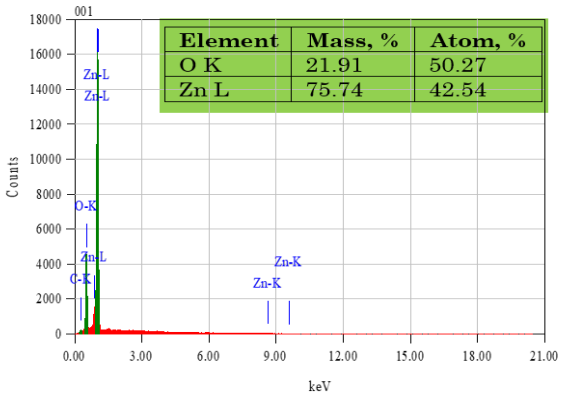

b

Fig. 4 – (a) FESEM image of ZnO thin film and the inset show spherical ZnO nanostructures covering deformed flower-shaped structures (b) corresponding EDS with suitable indexing

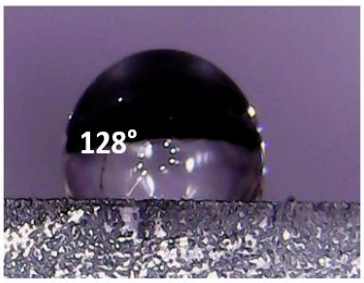

a

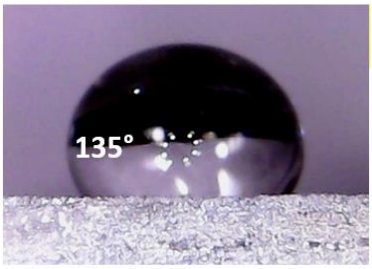

b

Fig. 5 – Measurement of hydrophobicity in terms of water contact angle (CA): (a) ZnO 2 h at 400 °C and (b) ZnO 2 h at 500 °C

An increase in the contact angle (Fig. 5) from 128° to 134° is observed when the ZnO films deposited on an

aluminum substrate undergo heat treatment at 400 °C and 500 °C, respectively. The contact angle (θ) values found for the two treated films are > 90°, which shows the hydrophobic nature of the films studied. This behavior could be attributed to the effect of layer density and surface roughness [18]. The same result was observed by Sanjeev et al. [19], who confirms the hydrophobic character of ZnO films deposited on glass substrate as a function of the annealing temperature between 200 °C and 400 °C. Therefore, the annealing temperature increases the roughness of the ZnO films, which is confirmed by the work of Husna et al. [20].

4. CONCLUSION

In the current study, thin layers of electrodeposited Zn were thermally oxidized on an aluminum substrate to create a hydrophobic surface. The aluminum substrates were immersed in the aqueous solution of zinc acetate and were subjected to a continuous voltage (–10 V DC). The structural results (DRX) revealed that the treated films have a hexagonal structure of the Wurtzite type due to the existence of the most intense peak relating to the orientation (100). Crystallite size is calculated using the Debye-Scherrer formula, an increase in D between 19.529 nm to 21.324 nm as a function of Ts = 400 °C and 500 °C, respectively. The morpho-logical analysis shows that the surface is composed of deformed micrometric structures in the shape of a ZnO flower. The contact angles measured are greater than 90° for all the samples treated at 400 °C and 500 °C, confirming the hydrophobic nature of all the films obtained, with a high value of θ = 135° for the film treated at 500 °C.

REFERENCES

1. N. Guermat, W. Daranfed, I. Bouchama, N. Bouarissa, *J. Mol. Struct.* **51**, 129134 (2021).
2. W. Darenfad, N. Guermat, K. Mirouh, *J. Nano- Electron. Phys.* **13**, 06016 (2021).
3. Y. Kang, F. Yu, L. Zhang, W. Wang, L. Chen, Y. Li, *Solid State Ionics.* **360**, 115544 (2021).
4. T.M. Schutzius, S. Jung, T. Maitra, *Nature* **527**, 82 (2015).
5. G.B. Darband, M. Aliofkhazraei, S. Khorsand, S. Sokhanvar, A. Kaboli, *Arab. J. Chem.* **13**, 1763 (2020).
6. A.M.A. Mohamed, A.M. Abdullah, N.A. Younan, *Arab. J. Chem.* **8**, 749 (2015).
7. F. Ahmed, *Adv. Mater. Lett.* **2**,183 (2011).
8. J. Serrano, F.J. Manjón, A.H. Romero, A. Ivanov, M. Cardona, R. Lauck, *Phys. Rev. B* **81**, 174304 (2010).
9. N. Bouhssira, S. Abed, E. Tomasella, J. Cellier, A. Mosbah, M.S. Aida, M. Jacquet, *Appl. Surf. Sci.* **252**, 5594 (2006).
10. N. Guermat, W. Daranfed, K. Mirouh, *Annales de Chimie - Science des Matériaux* **44**, 347 (2020).
11. A. Ashour, M.A. Kaid, N.Z. El-Sayed, A.A. Ibrahim, *Appl. Surf. Sci.* **252**, 7844 (2006).
12. P. Bindu, S. Thomas, *J. Theor. Appl. Phys.* **8**, 123 (2014).
13. J.G. Quiñones-Galván, I.M. Sandoval-Jiménez, H. Tototzintle Huitle, L.A. Hernández-Hernández, F. De Moure-Flores, A. Hernández-Hernández, E. Campos_Gonzalez, A. Guillén Cervantes, O. Zelaya Angle, J.J. Araiza-Ibarra, *Res. Phys.* **3**, 248 (2013).
14. B. Sahin, T. Kaya, *Mater. Sci. Semicond. Proc.* **121**, 105428 (2021).
15. R. Cusco, E. Alarcon-Llado, J. Ibanez, L. Artus, J. Jimenez, B. Wang, M.J. Callahan, *Phys. Rev. B* **75**, 165202 (2007).
16. B. Hadzi, N. Romcevi, M. Romcevi, I. Kuryliszyn-Kudelska, W. Dobrowolski, U. Narkiewicz, D. Sibera, *Opt. Mater.* **58**, 317 (2016).
17. L. Bergman, X.-B. Chen, J. Huso, J.L. Morrison, H. Hoeck, *J. Appl. Phys.* **98**, 093507 (2005).
18. N. Guermat, W. Darenfad, K. Mirouh, M. Khalfallah, M. Ghoumazi, *J. Nano- Electron. Phys.* **14** No 5, 05013 (2022).
19. S. Sanjeev, D. Kekuda, *IOP Conf. Ser.: Mater. Sci. Eng.* **73**, 012149 (2015).
20. J. Husna, M.M. Aliyu, M.A. Islam, P. Chelvanathan, N.R. Hamzah, M.S. Hossain, M.R. Karim, N. Amin, *Energ. Procedia* **25**, 55 (2012).